

# Cause of Starship crash on first flight

Yu. I. Lobanovsky

## Summary

Based on SpaceX video stream of April 20, 2023 about Starship launch, as well as available telemetry, it is shown in this work that on entire part of the trajectory where controlled flight took place, this rocket experienced sharp acceleration fluctuations with a period of 12 seconds, expressed in form of at least 10 pairs of narrow spikes, a sharp drop in acceleration to almost 0 at first, and then very sharp increase of it.

This behavior of Starship is caused by previously unknown in rocket technology interaction of longitudinal self-oscillations of Pogo-type with rocket control system. These self-oscillations were excited by hydroacoustic pressure disturbances in fuel lines of rocket engines. A numerical model has been created at first for calculating such hydroacoustic oscillations with pressure discontinuity at pump, and their interaction with own longitudinal vibrations of Starship hull have been analyzed. It was also shown that these intense longitudinal vibrations with a frequency of about 6 Hz were activated by hydroacoustic oscillations, frequency of which was on 3 or 4 times less, that is they had multiplicity 3 – 4.

It follows from the calculations that engine throttling increases the frequency of hydroacoustic oscillations, and the response of the control system to intense Pogo-type oscillations – decreasing of engines thrust, transfer this oscillating system from the vicinity of initial multiplicity point to even more dangerous point of lower multiplicity, that led to a never before seen behavior of rocket system with the emergence of periodic double spikes of longitudinal acceleration, which ultimately caused Starship crash.

**Keywords:** *Pogo, self-oscillations, Starship, accident, frequency, excitation, hydroacoustic oscillations, own oscillations, multiplicity*

## Symbol list

$c$  – speed of sound  
 $c_0$  – speed of sound in unbounded medium  
 $D$  – diameter  
 $E$  – modulus of elasticity  
 $E_f$  – modulus of liquids elasticity  
 $E_w$  – modulus of elasticity of tube wall material  
 $F$  – function  
 $f_n$  – frequency of hydroacoustic oscillations  
 $f_e$  – own frequency of rocket hull  
 $k$  – rigidity of oscillation system  
 $L$  – length  
 $L_a$  – acoustic length of oscillatory circuit  
 $L_{eq}$  – equivalent length of oscillatory circuit  
 $m$  – mass  
 $n$  – number of acoustic oscillations mode  
 $p$  – pressure  
 $T$  – temperature  
 $\delta$  – wall thickness  
 $\kappa$  – scaling parameter  
 $\rho$  – density  
 $\theta = (\pi ED\delta)/(mL)$

## I. Introduction

As you know, on April 20, 2023, first test launch of Starship was carried out from launch site at private Star Base spaceport in the vicinity of Boca Chica Texas settlement on the Gulf Coast. In accordance with the practice of SpaceX, which is the creator of this new promising and potentially reusable system, this launch was shown live in real time, and some of its flight data, including flight speed, were continuously shown. And while watching this video, the author of this work noticed that speed of the rocket system almost stopped increasing periodically, that is, there were long-period longitudinal oscillations of the rocket in flight. Moreover, they were accompanied by engines shutdowns, explosions, fires in compartments and telemetry failures. Eventually, Starship lost control and was blown up. It is quite obvious that such a picture could not be caused by anything other than some type of self-oscillation, although their period turned out to be unprecedentedly low for rocket vehicles.

Author has repeatedly developed theories describing various types of self-oscillations, so he decided to understand what he saw on the screen. By end of May, the desired theory as a whole had been created, and 45 days after first flight of Starship, at the beginning of June, this work was completed. By that time, the second launch of the rocket system was expected to take place before the end of the summer, so the author decided to wait to make this work public until it was confirmed, already obvious to everyone, in the form of second accident. However, numerous delays of this event due to lack of launch permits from various US government authorities are pushing it back indefinitely. Therefore, the author decided to publish a short version of this work now. Apparently, now there is actually time to carry out measures that would prevent a second accident of Starship for the same reason as the first, and, perhaps, would allow it to ultimately not repeat the mournful path of the Soviet N1 lunar rocket. "There would have been no happiness, but misfortune helped".

## II. Double spikes and key events of Starship first test flight

On April 20, 2023, the first test launch of Starship, consisting of first stage – Super Heavy B7 and second stage – Starship S24, vehicle of the same name, was carried out from launch position at Starbase – private spaceport on the Gulf Coast.

According to the results of testing the power plant at the start, only 30 out of 33 engines were turned on [1]. From the analysis of further information obtained, it follows that these were E1 – one of three central engines, and two outer ring engines – E26 and E27. At the 27th second of flight, an alleged "explosion of unknown nature" occurred, as a result of which protective screens of four engines of outer ring (E17 – E20) were "knocked out", and communication controller of one of these engines was lost [2]. At the 38th second of the flight, 11 seconds after, first engine from 30 operating was switched off. It was E18 engine from outer ring, one of that which had lost protective screens.

At 60th second of the flight, E22 engine stopped working, and no later than 67th second, E-18's neighbor, E19 engine, switched off, but perhaps not completely (that is, it functioned in low thrust mode). Around 90th second, another one central engine E2 stopped, and at 99th second sixth outer ring engine, E23, switched off also. Approximately at 110th second, E23 engine appears to turn on again, judging by the iconography, although the outer ring engines do not have the means to start in flight. At 112th – 113th seconds of flight, a powerful burst of flame was noticed, and at 122th seconds, entire first stage was engulfed in fire [3]. At that moment, the rocket began to perform an off-design pitching maneuver, which eventually turned into a somersault, which, as a result, turned into a full-fledged somersault, or from a different point of view, this maneuver can be called a "dead loop" aerobatics. At the same time, according to Elon Musk, control of the engine thrust vector was lost at 85th second [2]. Then, without collapsing during the somersault, the rocket made two more such maneuvers up to running out of fuel. At ~ 200th second of the flight, the vehicle was blown up so that its fragments would not go beyond the pre-planned fall zone of the first stage, and 40 seconds after that, having entered the denser layers of the atmosphere, it finally fell apart into separate fragments.

Quite significant destructions of starting position was also recorded [2], however, according to Elon Musk, there is no evidence that any engine could be damaged during launch from debris formed because of concrete coating destruction of the starting position.

This test flight scenario of Starship was compiled on the basis of two interviews with Elon Musk [1, 2], SpaceX stream footage [4], iconography of this stream showing the number of operating engines, telemetry information [5, 6] and chronology of events [3, 7]. And, we are primarily interested in something else – the reason that caused this anomalous operation of Super Heavy – the first stage of a giant rocket system.

Even while watching SpaceX stream, which showed in real time the preparation for launch, launch, flight and explosion of Starship system [4], in the window demonstrating acceleration rate, we noticed strange periodic cessations (or almost cessations) of speed increase in short moments of time (2 – 3 seconds), after which the periods of its rapid increase began again. All this were happening almost from the start, long before the implementation of all these impressive somersaults demonstrated by this rocket system in the last 1.5 minutes of its existence.

These observations are illustrated in Fig. 1, which is a plot of flight speed versus time. This plot was posted on NSF forum a day after launch [5]. Here, flight speed is measured in kilometers per hour; time is in seconds. Blue curve is data from the first stage – Super Heavy, purple – from the second stage of Starship, two vertical blue straight lines and two small blue triangular protrusions are telemetry transmission failures. Judging by the data given, there were 4 very short transmission failures from Super Heavy, and none during the transmission of information from the second stage of Starship. This means that these periods of cessation of speed growth existed in reality, and they were not caused by telemetry failures in any way (but the opposite is quite possible and even, as shown by further analysis, almost obvious). Small discrepancies in the data from these two stages in the last leg of the flight, when Starship made quick flips and rotations, are obviously quite objective for the sensors, apparently

separated by several tens of meters (length of Starship system is 120 m). At the same time, before the start of such maneuvers, both sensors produced practically identical data, with the exception of moments of short-term failures of sensor located on Super Heavy.

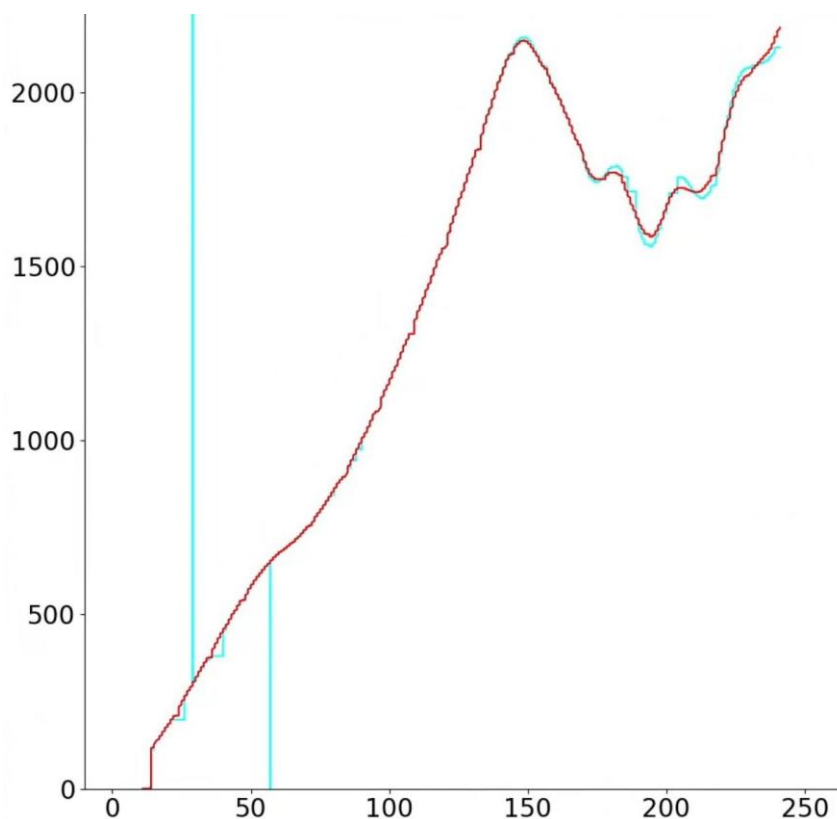


**Fig. 1 – Dependence of the rocket system speed on flight time [5]**

But much earlier, 2 hours and 15 minutes after the explosion of this launch vehicle, telemetry from another source appeared on the network with combined data on its four parameters: rocket acceleration (in  $\text{cm/s}^2$ ), speed (in  $\text{m/s}$ ) and height flight (in hundreds of meters), as well as the number of operating engines (in the graph, this number is multiplied by 10 to obtain a comparable scale of the curves), see Fig. 2 [6]. Failures of engines E19 and E2 on this graph, as well as in the corresponding information window of the stream, were not recorded.

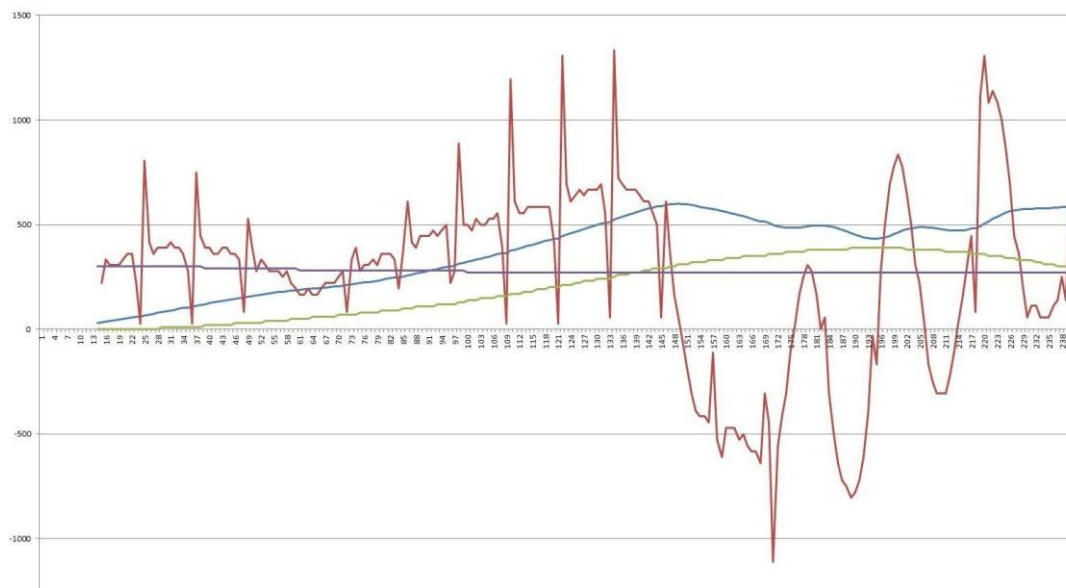


**Fig. 2 – Speed, acceleration, height and number of operating engines of Starship [6]**

On Fig. 2, in the area of the system’s motion without somersaults, 10 periodically repeating double multidirectional acceleration peaks (superspikes) are visible, and the trajectory breaks down at last spike, and Starship switches to random somersaults with rotations.

Our main interest was focused on telemetry from the beginning of its demonstration (about 15th second of the flight) to about 145th second, up to which the flight according to these data took place, at least with holding (to one degree or another) of a trajectory close to the given one. We see that in this part of the acceleration graph there are very sharp peaks, first directed downward, almost to 0, and then sharply upward until about a doubling of the current acceleration. It was at these moments that the speed seemed to freeze on the scoreboard during the stream. They also correspond to steps on the velocity graphs in Fig. 1, constructed from both first and second stages of Starship data. Such peaks on charts are usually called spikes, but here these spikes are very peculiar – every 12 seconds a pair of down-and-up spikes appeared in concert, only in the interval of 50 – 70 seconds there was no of them.

Further analysis showed that, in fact, the real process differs significantly from what is displayed on the graph with a data presentation period (quantization) of 1 second, since the characteristic frequency of oscillation process which generates these spikes should be, as shown below, about of 6 Hz. Therefore, its characteristic time is on the order of  $10^{-1}$  seconds, and in order to obtain a real picture, the data quantization period should be significantly shorter, that is, on the order of  $10^{-2}$  seconds. We also note that the skipping of one spike corresponds to moment of Super Heavy power plant throttling, which followed from flight plan and is directly seen from the acceleration in Fig. 2. During normal acceleration of the system, the moment of passage of maximum velocity head, when the thrust of Super Heavy should be decreased, is 55th second of the flight [7], but in reality this time corresponded to 77th second. From this it is clear that its power plant is involved in the occurrence of spikes. They, as will be shown below, are a superprocess in relation to the primary process, so these double spikes (due to the fact that they were first recorded on Super Heavy) can be called superspikes.

In the meantime, it immediately becomes obvious that almost all of the above significant events occurred 1 – 2 seconds after superspikes, so that one event that is not quite exactly defined in time, E2 engine shutdown (about the 90th second), can naturally be associated with the fifth superspike (83 – 87 seconds of flight). An event that did not seem to be directly related to superspikes was the shutdown of E19 engine, however, its protective screen was knocked out at the second superspike, and neighboring E18 engine had already stopped working by that time. Then, for example, a fire could start, due to which E19 stopped a little later.

### **III. Pogo oscillations are one of the reasons for anomalous behavior of launch vehicles**

So, it is quite natural to assume that the root cause of all or almost all the problems of Starship that have arisen in flight are the superspikes described above, which are a specific oscillation process that has not previously been encountered in rocket technology. Period of this oscillation process is 12 seconds. With reduced thrust of the first stage propulsion plant, one superspike did not appear at the right time, and the interval between successive superspikes was doubled. In total, 10 superspikes can be reliably noted until the moment when this rocket system was still making a more or less controlled flight. From the fact that this periodic process directly affected the movement of the entire rocket system, and also from the fact that superspike did not arise with reduced thrust, it clearly follows that this process is very similar to long-known Pogo oscillations, which previously repeatedly led to strong vibrations of rocket vehicles, shutdown of their engines or even destruction of vehicles in flight.

Pogo-type oscillations are dangerous self-oscillations of rockets with a frequency, usually 5 – 20 Hz, which can arise in a system consisting of elastic along the longitudinal axis rocket hull and liquid in its fuel lines. Rocket engines that consume fuel from main pipelines respond to fluctuations in its consumption, which causes thrust fluctuations, creating in turn elastic hull vibrations that affect fuel consumption. Thus, a positive feedback is created between the fluctuations of the liquid (one of the fuel components, usually an oxidizer) and an elastic solid body (rocket structure or some of its elements, for example, an engine mounting support that transfers engine thrust to its structure) [8]. And if frequencies of these two types of oscillations are close, they become undamped, and in many cases their rapid growth can be observed when the energy supply to this process from power plant operation exceeds its natural dissipation. In this case, increase in oscillation amplitude will continue until dissipation in the system is equal to supply of energy to it from an external source (in the case of Pogo – energy of burning fuel), or until the system changes its mode of operation (the engines will be turned off), or it will not cease to exist (rocket vehicle will collapse).

At first glance, it seems that the process we are considering is similar to Pogo oscillations in their stationary (non-growing) version. However, characteristic Pogo frequency is about 5 – 20 Hz, and frequency of the process under consideration is ~ 0.1 Hz, that is, 1.5 – 2 orders of magnitude less. The quantitative difference is so great that it cannot but be qualitative. And it cannot be explained in any way by the unprecedentedly large size of Starship launch vehicle – in terms of launch mass, it is slightly more than 1.5 times larger than Saturn V rocket. No rocket hull can have an own frequency of oscillation of the order of 0.1 Hz. In addition, normal self-oscillatory process looks completely different than what can be seen in Fig. 2 – usually there is an increasingly accelerating enlargement in amplitudes over several tens of oscillations, until either it stabilizes, or this process stops itself. A record of one such self-oscillatory process that occurred at the end of the second-stage boost phase of Saturn V rocket during launch of Apollo-13 lunar manned spacecraft into orbit is available to public, see Fig. 3.

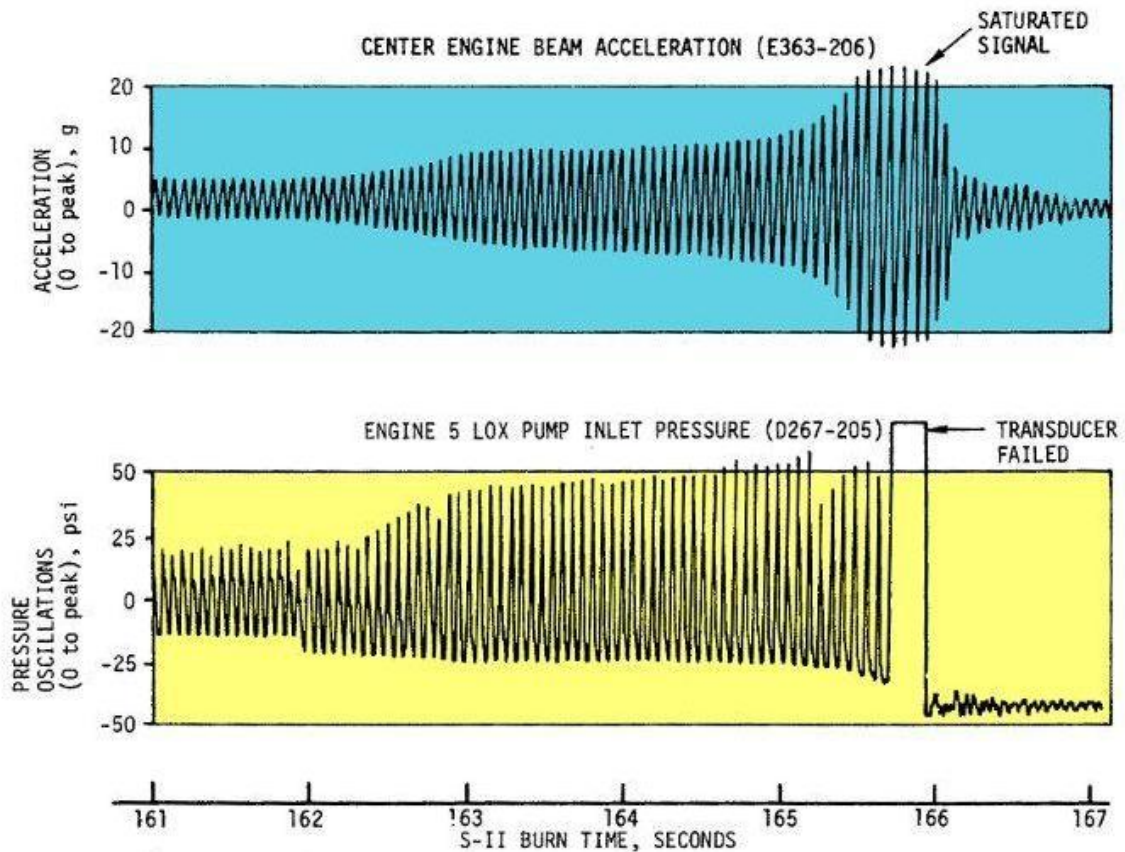


**Fig. 3 – Acceleration oscillations of Saturn V rocket S-II stage and pressure at the inlet to oxidizer pump of central engine J-2 [9]**

In this flight of Saturn V rocket, shortly before completion of its second stage, Pogo oscillations occurred with a frequency of  $\sim 16$  Hz in acceleration and  $\sim 15$  Hz in pressure (see Fig. 3), associated with the operation of its central hydrogen-oxygen rocket engine J-2. In about 3.5 seconds, they reached such a level that the instantaneous accelerations of corresponding sensor went beyond the range of its operation, and, according to estimates, exceeded 30 g. Pressure sensor at the inlet to oxidizer pump also failed due to off-design levels of pressure peaks, but the control system managed to turn off this engine, and then due to a slightly longer operation of four remaining J-2 engines, a bunch of the second, third stages and Apollo-13 spacecraft reached staging point at the required speed. The third stage with the same J-2 engine launched twice and completed the program without any problems, sending crew of Apollo-13 lunar spacecraft to new deadly adventures [9].

The liquid oscillating in pipes in this incident, as follows from its description, was oxidizer – liquid oxygen, and elastic solid body – sub-frame, on which 5 J-2 hydrogen-oxygen rocket engines were fixed. At the same time, the process started only in one, the central engine, which obviously differed from the other four in the length of the line from tank with liquid oxygen located directly above them.

In the described self-oscillatory process, the excitation from stationary state to its termination occurred in 50 – 60 oscillations over a time of about 3.5 – 4 seconds. And its duration has already turned out to be commensurate with the intervals between superspikes we are considering as 12 seconds. Of course, these times differ by a factor of 3 – 3.5, however, the rate of self-oscillations development depends both on the frequency of oscillations and on the rates of energy supply and dissipation (determining damping decrement or increase increment), which can vary greatly in different rocket designs. In addition, the bundle of second and third stages of Saturn V rocket and Apollo spacecraft differ from the Starship system by an order of magnitude in terms of mass – cannot this affect the characteristic times of the processes under consideration? From the foregoing, we can conclude that superspikes as such do not exist in reality. They appear only as a reflection of a real self-oscillatory process when information is quantized by 2 orders of magnitude less than is necessary for its full description.

Self-oscillation process, called after 2 decades as Pogo oscillations, and sometimes arising during the acceleration of rocket vehicle, was noticed even during launches of German V-2 rockets from Peenemünde test site, but then it was rather weak, and constructor of these rockets Wernher von Braun decided it to ignore. For the first time, rocket designers encountered it at the turn of the 50s and 60s of 20th century (in the USSR when launching a three-stage version of "lunar" R-7 rocket in the fall of 1958, and in the USA – when testing a manned version of



Titan-2 ballistic rocket missile in 1962) [8]. At the same time, in the United States, the term "Pogo oscillation" appeared to describe it by analogy with the children's jumping toy popular then in the West, which is a metal tubular stick with a spring, a footrest and handles to hold on to.

As is known, a full-fledged theory of Pogo-type oscillations of rocket systems still did not exist, but it was soon realized that in order to prevent them, it is necessary to make sure that the main modes of hull elastic vibrations or its element involved in this process, and hydroacoustic oscillations would be sufficiently different in frequency. To do this, as a rule, after obtaining calculated or empirical data on the first mode of longitudinal vibrations of rocket structure and empirical data on liquid oscillations, hydraulic dampers were inserted into the fuel lines, which significantly reduced the frequency of hydroacoustic oscillations. Sometimes they did the opposite – for example, to suppress Pogo process on UR-100N ballistic missile, after this rocket was put into service, it was necessary to put loads on an elastic suspension tuned to "anti-resonance" with a Pogo frequency [8].

#### **IV. Do as needed what you can do, and do how you can what is needed**

Since there is very little information about the sequence of oscillation processes that occurred on April 20, 2023 with Starship, and also because there are no definite data on design of its first stage – Super Heavy, in which the described process arose, it is necessary to involve data on other more detailed processes of this type and designs, and try to understand the most important characteristics of not one Pogo cycle, but all of them. This requires at least elements of Pogo-type oscillations theory, which has not yet existed, primarily, apparently, because there were no ways to calculate the oscillations of liquid in fuel lines of rockets due to the fact that in them there are units (pumps and turbines) that radically affect this process. If we can calculate the frequency of these hydroacoustic oscillations, then we can compare it with the frequency of rocket structure main mode of longitudinal oscillations and understand what happens without costly and accident-prone launches of this rocket. And then, using this knowledge, it will be possible to make decisions on finalizing this rocket system.

In order to deal with this April incident "on the tip of a pen", a method should be found for calculating hydroacoustic oscillations in rocket engine pipelines. And, fortunately, there is a quite suitable base for this, developed in a completely different field of engineering activity – in hydropower. Therefore, following the motto given in the title of this section of article and attributed to Lev Landau, we will do how we can what is needed, using already developed theory of hydroacoustic self-oscillations occurrence in penstocks of hydroelectric power plants [10 – 12].

As it turned out, these self-oscillations in penstocks and Pogo processes, being at least half different in their physical nature, are almost completely identical in their mechanical essence. In both cases, there are 2 oscillatory circuits, processes in which reinforce each other due to interaction between them through an energy object, operation of which depends on these processes. Therefore, part of energy it produces is invested in oscillations, and they are amplified. In a rocket vehicle, this energy object is a liquid-propellant rocket engine (LPRE); in penstocks of a hydroelectric power plant (HPP), it is a hydraulic unit, that is, a turbine with electric generator. In both cases, one of the processes is fluctuations of the liquid in the pipe, and the other is elastic vibrations of the structure (in the "rocket" version), or (in the "hydropower" version) – usually, vibrations of cavitation cord that occurs in the penstock behind the radial-axial turbine on non-optimal mode of operation. At the same time, the process of hydroacoustic oscillations in hydropower is excitable, and in rocket technology, on the contrary, it is exciting, if it is possible to consider such unambiguous definitions to describe interrelated and closely interacting processes. If the frequencies of exciting and excited processes are close to each other, then growing self-oscillations can occur, which usually ends, at best, with shutdown of the energy object (LPRE or hydraulic unit), and at worst, with the destruction of the entire system in which this process arose. So, for example, were destroyed in September and October 1958 during the first attempts to launch spacecraft to the Moon two R-7 rockets [8], and the turbine hall of Sayano-Shushenskaya HPP with 75 human casualties in August 2009 [11, 12].

In connection with the above, we first briefly consider the oscillations of a liquid in a pipe. As has been known since the second half of the 17th century, in a pipe, both with open and closed ends, filled with a continuous medium, standing waves can occur, creating oscillations of the continuous medium of maximum amplitude. The set of frequencies of these waves is infinite, but there is a standing wave of minimum frequency, amplitude of which is the largest. For a pipe that is open at both ends (this is the case of a hydroelectric power plant penstock) or closed on both sides, the minimum frequency corresponds to a standing wave, half the length of which is equal to the length of this pipe. For a fuel component supply line to a liquid rocket engine, the model describing this process must correspond to a pipe open at one end (where the fuel component enters from tank) and closed at the other (where it enters the main combustion chamber of the engine or its gas generator). In the combustion chamber, liquid turns into a weakly ionized gas; acoustic disturbances in the liquid practically do not pass through the liquid-gas interface, but are mainly reflected from it, as from a solid wall. Then the minimum oscillation frequency in such a pipe corresponds to a standing wave, a quarter of length of which is equal to the length of this pipe:

$$f_n = \frac{nc}{4L_{eq}}, \quad (1)$$

where  $f_n$  is the frequency of the mode  $n$ ,  $c$  is speed of sound in a continuous medium filling the pipe,  $L_{eq}$  is the equivalent length of the pipe, i.e. such that formula (1) or another similar formula (for example, half-wave) is correct even for less trivial cases than a pipe without any internal elements. For an empty (without internal elements) pipe with closed ends  $L_{eq} = L_a = L$ , where  $L_a$  is the acoustic length of the pipe and  $L$  is its physical length. If at least one of the ends of the pipe is open, its acoustic length becomes slightly longer than the physical one, due to the relatively weak effects associated with the emission of sound from the open end [11]. Now, at preliminary stage of considering the problem, we will neglect this effect, which increases the acoustic length of the pipe compared to the physical length by about 2/5 of its diameter for each open end. This does not make any sense in conditions when we do not know exactly the actual lengths of fuel pipelines of any launch vehicles considered below.

## V. Features of flow hydroacoustic oscillatory circuits with internal elements that take energy from the flow or introduce it into the flow

If elements are introduced into the hydroacoustic oscillatory circuit that take energy from the flow or introduce it into the flow, such as turbines or turbopumps, then various relationships between the physical and equivalent lengths of the circuit are possible. Particularly large differences between them are obtained on "rocket" quarter-wave oscillatory circuit at large energy rises, or, which is practically the same, in the case of relatively slow flows of an incompressible fluid, its pressure rises. In such cases, the difference between  $L$  and  $L_{eq}$  is quite possible by almost an order of magnitude, see below.

Acoustic oscillations in a pipe with a flow energy (pressure) stepped difference are described by a system of two nonlinear differential equations obtained by Fourier method from a one-dimensional wave equation for the velocity potential under certain conditions at the ends of the pipe and at the boundary of parameters discontinuity [10, 11]. It is neither the time nor the place to describe in detail both derivation and methods for solving this system of equations, especially since it was derived for a penstock, that is, a circuit with open ends and with a turbine – active element that takes the flow energy. True, the same equations were just as successfully used to calculate penstock of pumped-storage hydro stations, in one of two possible modes of operation in which the turbine unit is a pump. So, in essence, the only difference between "hydropower" and "rocket" models is the boundary condition at one of oscillatory circuit ends, which, in the case of the "rocket" model, leads to a quarter-wave base (and, apparently, the only possible) oscillation mode.

In this system of equations, there are 2 dimensionless determining parameters, the first one, which reflects the height of pressure drop on the "step", simulating the operation of turbine unit, mainly determines frequency of hydroacoustic oscillations, and the second one is proportional to the derivative of undisturbed pressure with respect to flow rate, and determines the growth rate or damping decrement of oscillations, and has a little effect on the frequency. Therefore, as shown by numerous calculations of acoustic characteristics in penstocks, for a preliminary frequency analysis of oscillatory circuit, it is quite possible to assume the second parameter to be 0.

Amplitudes of first half-wave oscillations mode are shown on Fig. 4 in penstock of model hydroelectric power plant, similar in characteristics to Sayano-Shushenskaya HPP with rounded values of main parameters for ease of demonstration. Flow of water is from left to right. Solid black curve with step at the locations of turbine in the penstock is the result of solving the above mentioned system of equations. The jump in the amplitude of oscillations on the step is exactly the same as the jump in the stationary (not oscillatory) flow pressure. The blue dotted line corresponds to oscillations of the same frequency, but without an active element inside the penstock, that is, a wave, whatever it would be without a jump in parameters – a half-wave of equivalent length  $L_{eq}$ . The red dotted line is the upward continuation of oscillatory solution from the region behind the turbine – a half-wave of the same equivalent length, but with amplitude, the value of which is determined from the ratio of the amplitudes on the step. So the real wave is a stitching of these two identical in length, but different in amplitude, equivalent half-waves through a step – a pressure jump.

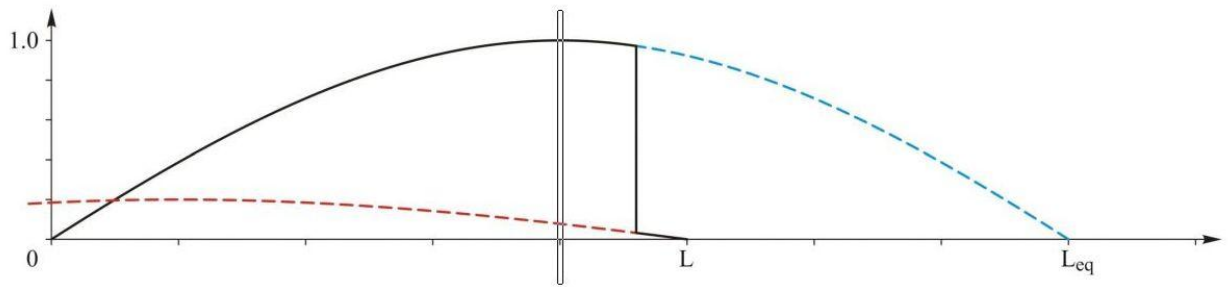


**Fig. 4 – Graph of the first (half-wave) mode acoustic oscillations amplitude in penstock of the model hydroelectric power plant and a cutout of a quarter-wave mode**

In Fig. 4 the section of penstock upstream of the turbine is longer than the section of penstock behind the turbine. The height of the pressure drop in Fig. 4 – 25:1, that is, a high water head of radial-axial turbine, modeled by a step, takes 96 % of its energy from the flow in the design mode. It can be seen that in the first case physical length of penstock is only 5/8 of the of equivalent penstock length without a turbine.

Let us now turn to the transformation of these results into a quarter-wave mode, which is characteristic in the case of Pogo-type oscillations. To do this, we divide the oscillation zone in Fig. 4 in half, and consider its right half. It is obvious that if a solid (for hydroacoustic oscillations) boundary is drawn through the middle of this zone, and appropriate boundary conditions are set, (left half of zone will be excluded from consideration), then the remaining half of solution will satisfy them – node of the oscillatory pressure will be located at the right open end, and in the middle, on new left border, will be maximum, as it should be on a solid wall. In this case, the boundary will be a solid wall only for acoustic oscillations, and the flow will freely cross it, making a phase transition. If you mentally change the direction of flow movement in the opposite – from right to left, then the step will turn from falling to increasing, that is, it will already simulate a turbopump. And then for this example, the ratio of physical length of the quarter-wave oscillatory circuit to the equivalent one will be, as can be seen from the diagram, 1:4.

In addition, it immediately becomes obvious that with an unlimited decrease in the length of high-pressure section in the fuel pipeline and an increase in the height of the pressure step, the ratio of equivalent circuit length to the length of real (physical) circuit will increase indefinitely. This means that on short fuel lines with high pressure rises, hydroacoustic oscillations will occur with frequency, which can be many times lower than what would be in them in the absence of a pump.

## **VI. Reconstruction of Saturn V first and second stages oxygen pipelines design characteristics from their Pogo oscillations frequencies**

Let us apply our version of hydroacoustic oscillations theory in a tube with an energy object inside it for the quarter-wave mode to real cases of Pogo oscillations in rockets with LPRE. In order to compare theory and experimental data, it is necessary to know 5 parameters: length of fuel pipeline from tank to pump and from pump to combustion chamber closest to it (main chamber or gas generator), pressure rise across the pump, frequency of oscillations and the speed of sound. Unfortunately, lengths of fuel lines sections indicated above are, apparently, only in the design documentation, which is not in the public domain. Remaining 3 parameters can sometimes be found. At the same time, by stitching hydroacoustic solutions of individual objects, using reasonable assumptions about their designs, it is possible, on the basis of calculations, to obtain quite certain lengths of fuel lines in order to analyze them for adequacy. If the obtained results are consistent with engineering ideas about design of objects, then the proposed method for calculating the frequencies of hydroacoustic oscillations in the fuel lines of a rocket engine can be applied in other cases.

So far, 2 incidents have been found with occurrence of Pogo oscillations that fit the above conditions: these are self-oscillations of AS-502 Saturn V S-IC first stage during second launch of rocket on April 4, 1968 [8], and the case of the same oscillations of AS-508 rocket's S-II second stage during eighth launch on April 11, 1970 [9], already mentioned above. In both incidents, as well as in all other cases known to us with Pogo oscillations on objects with kerosene-oxygen or hydrogen-oxygen rocket engines, oscillations always occurred in oxygen lines (total 5 incidents with R-7, Saturn V and H1 rockets), see [8]).

The first stage of Saturn V rocket used F-1 engines, while the second stage used J-2 engines. Despite the fact that fuel components in F-1 engine were kerosene and oxygen, and it was designed to work from surface of the Earth, and J-2 – worked on hydrogen and oxygen at low and zero external pressure, these engines, developed by Rocketdyne company almost at the same time, structurally seem to be almost twins, including the organization of their oxygen lines related to engine fittings (from the pump to the main combustion chamber).



Both of them have oxygen pumps located on the side of main combustion chamber and are connected to its mixing head through "LOX/Oxidizer dome" located above it. Estimation of engines F-1 and J-2 dimensions (their lengths are 5.64 m and 3.38 m, respectively, and diameters are 3.72 m and 2.07 m) [13, 14] showed that scales of J-2 and F-1 correlate approximately like 0.6:1. Therefore, the first condition for connection (condition 1) of hydroacoustic oscillatory circuits' parameters describing processes of Pogo-type in these two cases under consideration was as follows: length of oxygen line section from the pump to the mixing head for J-2 is 0.6 of the corresponding length for F-1.

Length of the line from tank to the pump, on the contrary, is determined by design of stage in which the engines are located. Diameters of the first and second stages of Saturn V rocket are the same. Designs of their engine compartments are approximately the same also [15, 16]. But J-2 engine that began to oscillate is a central one, without a pivot, and is located against the center of domed rear cap of oxygen tank. As the result, we will assume that its oxygen line is 1.2 times shorter than the same section of line in engine compartment of F-1 in first stage.

However, in the first stage S-IC, liquid oxygen tank is located above kerosene tank, the height of which is 13.4 m [15], and in the second stage S-II, liquid oxygen tank is directly above the engine compartment under liquid hydrogen tank. Therefore, the second condition for the connection of oscillatory circuits' parameters (condition 2) was that length of this section at the first stage was greater than at second, by the height of the tank with kerosene also, that is, by 13.4 m.

Pressure rise across oxygen pumps is known: at the inlet, the pressures were 0.45 MPa and 0.27 MPa for F-1 and J-2, respectively, and at the outlet of the pumps, 11.0 MPa and 7.68 MPa [17]. Thus, the slightly rounded ratio of the pressures at the outlet and inlet, that is, heights of the steps on Fig. 4 is 24.5:1 for F-1 and 28.5:1 for J-2. It makes no sense to determine these values more precisely, since the physical lengths of oscillatory circuits are determined from the approximate conditions for their matching, and it is more convenient to analyze somewhat rounded data.

To close data array, it is also necessary to determine speed of sound in the oxidizer lines, that is, in the flow of cryogenic liquid oxygen. Temperature of liquid oxygen in tanks is close to 90 K, pressure at the inlet to the pumps is approximately 0.3 – 0.45 MPa. Very detailed data on the speed of sound in liquid oxygen at various temperatures and pressures are given in source [18].

Numerical model, originally created to calculate the acoustic parameters in the water flowing in penstocks of HPP's, where speed of sound was constant along the entire length of the penstock, does not provide for a break in this speed at pressure break. Therefore, the calculations in this work were performed for the average speed of sound, defined as half the sum of speeds at pressures before and after the pump. This introduces a certain error into the results obtained, which can be eliminated in the future when the model is refined.

At the same time, it should be remembered that the speed of sound in a pipe is lower than in an infinite layer of liquid, due to the fact that the pipe deforms ("expands") when increased pressure is passing through the pipe. The speed of sound in an elastically deformable pipe is determined by the following formula (see [19]):

$$c = \frac{c_0}{\sqrt{1 + \frac{DE_f}{\delta E_w}}},$$

where  $c_0$  is the speed of sound in an infinite fluid,  $D$  is the pipe diameter,  $\delta$  is the thickness of the pipe walls,  $E_f$  is liquid modulus of elasticity,  $E_w$  is modulus of elasticity of pipe wall material.

In this case, the modulus of elasticity of liquids can be determined as follows:

$$E_f = \rho c_0^2, \quad (2)$$

where  $\rho$  is density of liquid through which the sound wave propagates.

This issue was carefully worked out when determining the speed of sound in water flowing through penstock of Sayano-Shushenskaya HPP. In the cold water of Yenisei River (as, for example, in Lake Baikal), sound propagates at a speed of about 1420 m/s (see [20]). However, according to the source [10], speed of sound in the water flowing through the massive steel-concrete penstock of Sayano-Shushenskaya HPP was 1350 m/s, that is, it was 5 % lower than in an unbounded liquid. So the speed of sound in propellant components of a rocket engine also depends on design parameters of lines through which they pass, and a more accurate estimate of this value can only be made

using data from the manufacturer of this engine. And we, in a first approximation, will estimate the decrease in speed in the oxygen lines of rocket engines considered below at the same 5 %, since, on one hand, rocket structures are lighter and more openwork, and, therefore, have less rigidity than hydraulic engineering objects, but, on the other hand, at  $T = 90$  K, elastic modulus of liquid oxygen  $E_f$  is two times lower than that of water at  $T = 277$  K. Under the conditions of interest to us, the modulus  $E_f \approx 2$  GPa for water and  $\sim 1$  GPa for liquid oxygen. In this case, it should be noted that the elastic modulus of liquid methane, also considered below for the occurrence of Pogo oscillations, is approximately the same as that of liquid oxygen,  $E_f \sim 1$  GPa (see [21]).

As a result of the joint solution of wave equation with a discontinuity of parameters at the location of pump for the above two sets of characteristics, under conditions 1 and 2 and at known frequencies of hydroacoustic oscillations, which were equal to 5.0 Hz at S-IC stage and 15 Hz at S-II stage [8, 9], the lengths of sections of oxygen lines from the pump to the combustion chamber ( $L_1$ ) and from the tank to the pump ( $L_2$ ) are uniquely determined. These calculated values are shown in Table 1 (in section S-II and in the middle row of section S-IC). In table  $L_3$  is the total calculated physical length of the oxygen lines,  $L_{eq}$  – the equivalent length of the oscillatory circuit (at a known frequency, it can be easily calculated by formula (1) with  $n = 1$ ),  $f_n$  is the frequency of hydroacoustic oscillations. In this case, speed of sound in the flow of liquid oxygen when solving the equations for F-1 engine was taken equal to 845 m/s, and for J-2 engine – 835 m/s.

**Table 1**

Rocket Stage Engine	c (m/s)	p <sub>2</sub> /p <sub>1</sub>	L <sub>1</sub> (m)	L <sub>2</sub> (m)	L <sub>3</sub> (m)	L <sub>eq</sub> (m)	f <sub>n</sub> (Hz)
<b>c = 845 m/s</b>							
<b>Saturn V S-IC F-1</b>	845	24.5	1.36	13.40 + 3.51	18.27	40.5	5.21
			1.51		18.42	42.3	5.00
			1.66		18.57	44.0	4.80
<b>c = 835 m/s</b>							
<b>Saturn V S-II J-2</b>	835	28.5	0.90	2.92	3.82	13.9	15.0

In this calculation, apparently, quite adequate lengths of the oxygen line sections were obtained for both stages of Saturn V rocket. At S-II stage, the length of pipeline from tank to pump is 2.92 m, from J-2 engine's pump to middle of its mixing head – 0.90 m. At S-IC stage, pipeline from oxygen tank to F-1 engine's pump is significantly longer – 16.91 m, due to the fact that it crosses kerosene tank, and average length of pipeline from pump to mixing head of combustion chamber is 1.51 m.

In reality, F-1 engine had 2 pipelines of slightly different lengths from the oxygen pump to the mixing head, which differed approximately by the diameter of the pump. In connection with this circumstance, for S-IC stage, calculations were given with lengths  $L_1$  that differed by  $\pm 0.15$  m from the result obtained in the joint calculation. In this case, oscillation frequencies shifted from the average value by  $\pm 4\%$ , see first and third rows of the S-IC section of Table 1.

Mixing of two close frequencies in "Oxidizer dome" should have led to oscillations at fundamental (carrier) frequency equal to  $\sim 5.0$  Hz – half sum of the component frequencies and beats with a frequency of  $\sim 0.2$  Hz (half difference of the component frequencies). That is, approximately every 5 seconds, the amplitude of liquid oxygen oscillations turned out to be very small, which should have prevented the development of self-oscillation process, which lasted in the interval of 100 – 130 seconds of flight (that is, during which about 150 oscillations had passed), until the completion of work first step. Perhaps it was these beats (of which there could be 5 – 6) that saved Saturn V rocket on that flight from more serious troubles than those that happened then to it.

At the end of this section, we note that the equivalent lengths of the oscillatory circuits from Table 1, that is, the lengths that waves with given frequencies would have in the absence of a pressure step, are 2.3 – 3.8 times greater than the actual lengths of oxygen lines. Since in the calculations of the oxygen lines parameters of these Saturn V two stages, according to the frequencies of Pogo processes and characteristics of engines, quite adequate results of fuel pipelines' lengths were obtained, it can be argued that verification of the proposed calculation method has been completed successfully.

## VII. Frequency estimations and analysis of hydroacoustic oscillations in oxygen lines of Super Heavy during Starship first flight

Let's move on to assessing the frequencies of hydroacoustic oscillations in the oxygen lines of Super Heavy first stage of Starship in the configuration corresponding to its first launch – after all, in all known cases of self-oscillations of Pogo-type, they were always previously initiated exclusively by liquid oxygen oscillations, if it was part of fuel pair.

Length of Super Heavy stage is 69 m [22], which is 2.8 times longer than that of S-II stage, but height of Raptor-2 engine (3.1 m) [23] is even slightly less than that of J-2. Oxygen tank on the stage is located under the methane one, directly above engine compartment. So it is unlikely that the length of Super Heavy oxygen pipelines will be significantly longer than that of S-II stage. Due to the extremely high compactness of Raptor-2 engine and the layout of the engine compartment of Super Heavy, we will assume that the length of the oxygen line section from the tank to the engine pump (section  $L_2$ ) is 3.0 m.

The oxygen pump is located atop of Raptor-2 engine directly above the combustion chamber of gas generator, producing oxidant gas for turbine. Therefore, this part of the line (section  $L_1$ ) must be significantly shorter than that of F-1 or J-2 engines discussed above. We take  $L_1 = 0.40$  m as the base value. However, we do not have the exact data necessary for the direct calculation of the oscillation frequency; therefore, options with lengths of 0.30 m and 0.50 m were also considered.

The pressure rise across the oxygen pump of Raptor-2 engine is 6 to 7 times higher than that of previously considered rocket engines. Pressure is 0.4 MPa at the inlet and 69.6 MPa at the outlet at 30 MPa in the main combustion chamber. Rounding up, we get that the pressure rise across the oxygen pump in this engine is 170:1. The engine is capable of operating with thrust throttling up to 20 % of nominal value [23]. And the reduction in thrust actually occurred in the trajectory part in the vicinity of maximum velocity head ( $Q_{max}$ ) zone, as well as during each superspike. Therefore, we estimate the frequency characteristics of the process when the pressure in the combustion chamber and, accordingly, at the oxygen pump decreases by 2 and 4 times ( $p_2/p_1 = 85:1$  and  $42.5:1$ ). It has been estimated (see [24]) that the lower end of Raptor-2 engine's throttling range is roughly equivalent to oxygen a pump pressure of 40:1. Consider also the technically impossible, but useful for formal analysis, level of 28.5:1, as in J-2. At the speed of sound  $c = 930$  m/s, obtained by averaging over pressure, and reduced by 5 % due to the elasticity of pipelines, calculations were made for three variants of Raptor-2 engine, and 3 degrees of throttling were added to each of them, see below Table 2.

It can be seen from it that the frequency of hydroacoustic oscillations in the oxygen lines of the first stage in flight on April 20, 2023, with the nominal operation of the engines, could very likely be from 9 Hz to 12 Hz. A more accurate conclusion can be obtained after providing real data of oxygen lines' lengths. But, as further analysis showed, for qualitative conclusions, all these uncertainties, in essence, have no meaning. The resulting conclusion is quite definite.

**Table 2**

Rocket Stage Engine	$p_2/p_1$	$L_1$ (m)	$L_2$ (m)	$L_3$ (m)	$L_{eq}$ (m)	$f_n$ (Hz)
<b><math>c = 930</math> m/s</b>						
<b>Starship Super Heavy Raptor-2</b>	170	0.30	3.00	3.30	19.6	11.9
	85				14.0	16.6
	42.5				10.1	23.0
	28.5				8.42	27.6
	170	0.40		3.40	22.6	10.3
	85				16.1	14.4
	42.5				11.6	20.1
	28.5				9.59	24.2
	170	0.50		3.50	25.2	9.21
	85				18.0	12.9
	42.5				12.8	18.2
	28.5				10.6	21.9

In the considered range of parameters, a decrease in the pressure rise across the pump by  $\kappa$  times leads to a decrease in the frequency of hydroacoustic oscillations by almost  $\sqrt{\kappa}$  times, therefore, if Pogo-type process of oscillations occurred at the nominal operation of engine, then its throttling leads to an increase in hydroacoustic oscillations frequency in oxygen tract and to breakdown of Pogo process.

It can also be noted that with such large pressure rises across the pump, effective length of oscillatory circuit can be  $\sim 7.2$  times longer than the physical one. Only in connection with this effect, the hydroacoustic frequencies turn out to be so low that, in principle, they can be commensurate with the frequencies of own longitudinal vibrations of the hull or its structures such as engine mounting support, which creates conditions for resonances, and, consequently, for excitation of Pogo-type self-oscillations.

Comparison of J-2 and Raptor-2 engines frequencies at the same pressure rises, as well as a comparison of calculated options for the second engine, show that a decrease in  $L_1$  (distance from the pump to the combustion chamber) ceteris paribus, as expected, leads to increase of oscillation frequency. And reducing the length  $L_1$  by  $\kappa$  times leads again to an increase in frequency by  $\sqrt{\kappa}$  times.

### VIII. Own longitudinal oscillations' frequency estimations of Saturn V and Starship hulls

After obtaining data on the frequencies of hydroacoustic oscillations in the oxygen lines of Saturn V and Starship rockets, in order to study the possibility of Pogo oscillation's occurrence, we need to know frequencies of the first mode of own oscillations in their hulls. For lunar rocket, this frequency is known, so let's try to build the simplest model for estimation such oscillations and verify it using these data.

Of all the classical models describing longitudinal oscillations of a rod, the model of rod oscillations with a fixed end and a load at its other end seems to be closest to the case of a rocket flight. In this case, the rod performs free oscillations [25]. Such a model may be closest to reality for a rocket standing at the start. But even in flight, the thrust force "props up" its tail end. Of course, in reality, the mass is distributed along the entire length of the rocket; in addition, it decreases in flight. But for rockets of longitudinal scheme, this reduction in mass occurs in their tail section, which has the least effect on the own frequency of the structure. At least, in the materials available to us, a single value of rocket's own frequency was usually given, regardless of which part of the acceleration trajectory the described events occurred. For example, as mentioned above, it is reported that "the own frequency of AS-502 Saturn V was 5.3 Hz" [8]. And we will follow the same approach.

During oscillations of the model system described above, in the case when the mass of the elastic rod is negligible compared to the mass of the load, the frequency of own oscillations  $f_e$  is determined by the formula:

$$f_e \sim \sqrt{\frac{k}{m}}, \quad (3)$$

where  $k$  is the rigidity of the oscillation system,  $m$  is its mass. It should be noted that the mass of the side walls of Saturn V and Starship rockets (for the first one, with longitudinal stringers reinforcing the walls), which play the role of elastic element, are about 1.0 % and 1.85 % of the starting masses of these objects.

In the case of vibrations of a thin-walled pipe, formula (3) can be reduced to the following form:

$$f_e \sim \sqrt{\theta} = \sqrt{\frac{\pi ED\delta}{mL}}, \quad (4)$$

where  $E$  is modulus of material's elasticity,  $D$  is tube diameter,  $\delta$  is thickness of its wall,  $L$  is its length,  $\theta$  is the abbreviation for the underlying set of parameters.

For dimensional reasons, for a more complex system than a weightless elastic longitudinal rod with a load at the end, the frequency should also be a function of the parameter  $\theta$ :

$$f_e = F(\theta) \quad (5)$$

Rockets, as a rule, differ from thin-walled pipes primarily in that the diameters and wall thicknesses of their stages can vary (the material is usually the same for all stages). In order to overcome this difficulty in calculations, we will use the average values of any parameter that varies along the length  $L$ . The details of these calculations are presented in the full version of the work, but we note that the length of the oscillatory circuit of the Saturn V rocket did not include the significantly more rigid capsule and emergency recovery system located at its upper end [26]. In

addition, the height of the F-1 engines, as well as the distance from their top to the sub-engine frame to which they transmitted their thrust, were also excluded from the nominal length of the first stage, since this part of the stage hull was not under load from the longitudinal force. As a result, the length of the longitudinal oscillatory circuit of Saturn V rocket was shortened by 10.1 m at the top and 6.1 m at the bottom from the nominal, and its value turned out to be  $L = 94.4$  m. The average estimated diameter of the rocket  $D = 8.65$  m, and the design wall thickness  $\delta = 3.50$  mm and  $\delta = 4.08$  mm with the coefficients of its thickening due to longitudinal ribs – stringers (about which exact data were not found) 1.5 and 1.75, respectively. The elastic modulus of aluminum alloy 7075, from which the hull of Saturn V rocket was made, is  $E = 71.7$  GPa [27]. Its starting mass  $m \approx 3.0$  kt.

The frequency of own longitudinal oscillations of Saturn V according to formula (4) with a coefficient of proportionality in it equal to 1, and with the indicated values of the parameters included in it will then be  $f_e = 4.9 - 5.3$  Hz with wall thickening coefficients due to stringers 1.5 – 1.75, respectively. From the fact that the latter value exactly coincides with data what was recorded for Pogo oscillations during the flight of AS-502 [9], we can conclude that under the boundary conditions implemented in flight, as well as with the considered set of parameters, the function  $F(\theta)$  from formula (5) should not differ too much from its expression for the simplest calculation option, that is, simply from the square root. Therefore, in the first approximation, to recalculate the frequencies of objects close to Saturn V, we can use formula (4).

Let's apply this approach to Starship rocket, which is considered to be much simpler than Saturn V, since it has a constant diameter along the entire length  $D = 9.0$  m (we will neglect small ogival part at rocket top). The only difficulty is that the exact thickness of the steel sheet that forms the hull of S25 second stage is unknown. Either it is equal to 4.0 mm, as in the first stage, or it has already been reduced to 3.0 mm, as was done with the SN7.2 prototype, with which a cryogenic test was carried out on January 26, 2021. Therefore, own vibrations of the hull were assessed for two average values of wall thickness –  $\delta = 3.57 - 4.0$  mm (so the average effective wall thicknesses of both rockets turned out to be very close).

Elastic modulus of 304L stainless steel  $E = 193 - 200$  GPa [28]. It is believed that the launch mass of Starship, made from 304L steel, in the first test flight was  $m \approx 5.0$  kt. However, it did not then carry a payload, the mass of which is claimed to be 0.15 kt, so the lowest estimate of its real launch mass is 4.85 kt. Estimated height is  $L = 116$  m by subtracting the height of Raptor-2 engines and the distance from them to the support structure to which they are attached. The own oscillations of the hull were evaluated at two average values of the wall thickness. Then the own frequency of longitudinal oscillations of the hull, recalculated from the frequency of lunar rocket, is estimated as  $f_e = 5.8$  Hz and  $f_e = 6.25$  Hz, respectively. With the mass of 4.85 kt, this frequency can even be about 5.7 Hz.

It is easy to obtain from formula (4) that with similar increase in the object and a fixed value of elasticity modulus, the frequency of own oscillations drops:

$$f_e \sim L^{-1} \sim m^{-\frac{1}{3}}$$

That is, if Starship was a large-scale copy of Saturn V, then, due to increase in launch mass, it would have its own longitudinal oscillation frequency  $f_e \approx 4.5$  Hz. The main reason that, despite the larger size, the frequency of the last rocket is higher than that of the first one is that the elastic modulus of 304L steel is 2.7 – 2.8 times greater than that of 7075 aluminum alloy. Saturn V allows us to assume that recalculation of its experimental data by formula (4) for a close object, which differs by a noticeably simpler design, gives sufficiently reliable results. In the limit, when recalculated from a frequency of 5.3 Hz, with the minimum value of  $\theta$  complex for Saturn V and maximum value for Starship, the oscillation frequency of the latter can rise to a value of  $f_e = 6.8$  Hz, which, in fact, begins to exceed even oscillation frequency (6 – 7 Hz [8]) of Soviet lunar rocket N1 a half the mass and had a rigid semi-monocoque design of an aviation rather than rocket type [29]. So the most likely own frequency of Starship hull is most likely no more than 6 Hz.

From the values obtained above of the own frequency of Starship hull longitudinal oscillations, it can be concluded that oscillations of Pogo-type in the event of disturbances with any of the previously calculated variants of Super Heavy stage oxygen lines cannot arise. This is due to the fact that the frequencies of hydroacoustic oscillations in the oxygen lines of Starship system, depending primarily on length of its  $L_1$  section, are in the range of 9.2 – 11.9 Hz. And, most likely, the frequency corresponds to reality, is close to the upper limit of the specified range. But until the exact lengths of the hydraulic circuits of Raptor-2 engine's fuel system will be obtained, it remains to use the evaluative data presented above.

However, they are enough. The highest estimate of own oscillation frequency of Starship hull is 6.8 Hz, and the minimum value of the oxygen line oscillation frequency is 9.2 Hz. The frequency difference is at least 30 %, but the excitation of self-oscillations of this type is possible, as a rule, only with a frequency difference of no more than 7 – 10 % (for example, in incidents with Saturn V rocket stages, it was within 5.8 – 6.5 %). Oscillations of Pogo-type cannot be excited in such a situation. The only possible option is vibrations of an important rocket structural



element, for example, a support structure on which first stage engines are mounted, but there is no evidence of possibility of something like this, and this assumption cannot be confirmed by anything.

Of course, when frequency of exciting oscillations is higher than frequency of excited oscillations, one should check the possibility of resonance in the next, in this case, the second mode of the excited oscillations. However, for the considered parameters, the second mode frequency of the model oscillation system is close to 150 Hz (see [25]). Therefore, it must be assumed that such a variant is completely excluded for a real system, and it remains for us to study the last remaining possibility – Pogo variant with hydroacoustic oscillations in methane pipelines of Super Heavy.

### **IX. Frequency estimations and analysis of hydroacoustic oscillations in methane lines of Super Heavy during Starship first flight**

Let us now estimate frequency of hydroacoustic oscillations in methane pipelines of Super Heavy. At first glance, it becomes clear that their frequencies will be many times lower than oscillation frequencies in oxygen lines due to the fact that length of fuel pipelines is greater than length of oxidizer pipelines, at least by the longitudinal dimension of oxygen tank, which is approximately 33.4 m. Moreover and a larger pressure rise at methane pump, which is 220:1 versus 170:1 at oxygen pump [23], also increases acoustic length of methane lines, and, therefore, additionally reduces frequency of hydroacoustic oscillations. Therefore, it immediately becomes clear that their resonance with hull vibration frequencies of the order of 6 Hz is completely excluded, and it would seem that no Pogo oscillations in Starship can occur in this variant. Therefore, one should look for some other explanations for the incident that happened on April 20, 2023.

But, nevertheless, we will calculate the possible of hydroacoustic frequencies in methane pipelines, and only after that we will decide what can and what cannot happen there. The required characteristics of methane were taken from the source [21]. Since the elasticity modulus of liquid methane under the conditions of interest to us is approximately the same as that of liquid oxygen, the corrections for the elasticity of methane circuit pipelines were taken the same as before – the speed of sound decreased by 5 %.

So, the length of low-pressure methane main pipeline section is close to 36.4 m: the height of oxygen tank, 33.4 m, is added to the previous length from the bottom of it to the engine pump of 3.0 m. From the pump, the pipeline goes to the engine cooling jacket, where its flows bifurcate in the vicinity of nozzles critical part – one of them enters the jacket of the main combustion chamber, and the second – into the nozzle jacket. Then they merge, and already their total flow goes to combustion chamber of methane gas generator (where some oxygen also comes in). And the lengths of these two paths differ markedly.

Without any design documents for Raptor-2 engine, it is quite difficult to estimate these lengths. Therefore, we went the other way – based on the fact that oscillations of Pogo-type arose during the nominal operation of the engine, we determine what lengths of the high-pressure circuit of methane pipelines allow these oscillations to exist, and then we evaluate the feasibility of such a circuit within the framework of the generally known engine design and its dimensions.

To calculate the frequency characteristics of such bifurcated methane main line, we use the experience of acoustic oscillations calculating in F-1 engine, where oxygen was also supplied to main combustion chamber in two ways, see Section VI. Preliminary estimates have shown that the frequencies of hydroacoustic oscillations in methane pipelines, which allow oscillations of Starship system Pogo-type to occur, are possible, but under one condition. It lies in the fact that the frequency of the hydroacoustic oscillatory circuit, which excites the process of self-oscillations of Pogo-type, should not be close to the frequency of the excited circuit, but a multiple of it (again, with some accuracy). It has long been known that resonance occurs not only when the frequencies of excitation and own oscillations of excited system are close, but also when these frequencies are multiplied. This means that the excitation frequency can be  $n$  times lower than the excitation frequency, where  $n = 1, 2, 3, 4, \dots$ . However, as it turned out, not all rocket designers know this fact. Otherwise, the problem of longitudinal oscillations in Soviet lunar rocket N1 fourth flight, which, most likely, led to its fourth and last accident, would not have remained unresolved [8].

Preliminary calculations have shown that in the nominal mode of engine's operation, when pressure rise across methane pump is 220:1, and at technically acceptable lengths of high-pressure sections of the methane line from the pump to the gas generator, in principle, fluctuations with a multiplicity of 3 or 4 are possible. And, accordingly, pairs of "short" or "long" sections of high-pressure methane pipeline may exist. The length of "short" sections pair is about ~ 1.5 m for a shorter line and ~ 3 m for a longer line. For "long" pipelines lengths are about 2.5 m and ~ 5 m, respectively. Of course, it can be said that the choice of pipelines pair with an essentially random ratio of their lengths ~ 1:2 is not the basis for any general conclusions. However, it is further shown that this ratio practically does not play any role – at least in the range of ratios from 1:2 to 1:1, it can be any, without affecting the qualitative conclusions.

The results of these calculations are shown in Table 3. In its last column are indicated (through slash) main (carrier) frequency of the resulting oscillations, which is the characteristic of hydroacoustic disturbance, and carrier beat frequency, equal, respectively, to the half-sum and half-difference of frequencies in the two pipelines of pair. The first group of two lines corresponds to own natural frequency of Starship hull  $f_e = 6.25$  Hz (see Section VIII). In this case, the quadruple frequency of hydroacoustic oscillations acceptable for the occurrence of Pogo will be equal to 6.0 Hz, and then it will be within the boundaries of self-oscillations excitation. The second and third groups of rows in Table 3 correspond to the cases when the quadruple and triple frequencies of hydroacoustic oscillations are equal to 5.55 Hz, which leads to rather small deviations from the own frequency of longitudinal oscillations of the hull  $f_e = 5.8$  Hz. It seems that the lengths of the second pair of methane lines from Table 3 are too large for the extremely compact design of Raptor-2 engine, and then we are left with a simple alternative – with a possible own frequency of the hull  $f_e > 6$  Hz, the multiplicity of excitatory hydroacoustic oscillations is 4, and with  $f_e < 6$  Hz it should be 3.

**Table 3**

Rocket Stage Engine	$p_2/p_1$	$L_1$ (m)	$L_2$ (m)	$L_3$ (m)	$L_{eq}$ (m)	$f_n$ (Hz)	
$c = 1495$ m/s							
<b>Starship Super Heavy Raptor-2</b>	220	2.25	33.4 + 3.00	38.65	214	1.75	1.50/0.25
		4.47		40.87	299	1.25	
		2.64		39.04	231	1.62	1.39/0.23
		5.20		41.60	322	1.16	
		1.46		37.86	173	2.16	1.85/0.31
		2.93		39.33	243	1.54	

It should be noted that frequencies and equivalent lengths of oscillatory circuits given in Table 3 make us recall the similar parameters of large hydroelectric power plants. For example, the own frequency of hydroacoustic oscillations in the penstock of Sayano-Shushenskaya HPP is  $f \approx 1.55$  Hz, and the acoustic length of this tube at the speed of sound in water  $c = 1350$  m/s is  $L_{ef} = 435$  m with its physical length  $L = 269$  m, and  $L_{ef}$  there is the length of half of the wave, but here the largest value  $L_{ef} = 322$  m is the length of its quarter. So hydroacoustic wave of variant with physical length of the methane pipeline in Super Heavy stage  $L_3 = 41.60$  m is 1.48 times longer than the wave in the penstock of giant Sayano-Shushenskaya HPP.

The higher the multiplicity, the weaker the excitation, that is, self-oscillations occur at a smaller discrepancy between exciting and excited frequencies, which means a lower probability of starting such a mode. For example, 18 incidents are known with excitation of self-oscillations in penstocks of HPPs, of which 13 occurred at resonance, that is, at a multiplicity of 1, 3 – at a multiplicity of 2, and 2 – at a multiplicity of 3. The excitation of self-oscillations at a multiplicity of 4 in hydropower has not yet been recorded [30]. Therefore, it can be assumed that of those considered, the "short" option, the third one in Table 3, has the closest proximity to reality. But even there, the wavelength is at least 0.8 of the wavelength in the penstock of Sayano-Shushenskaya HPP.

With the multiplicity of hydroacoustic oscillations 3 and 4 with own frequency of the hull, this oscillatory system (Starship) may have qualitative and, possibly, visible differences in its behavior. To consider this thesis, let us determine how the carrier frequency changes when the engines of system power plant are throttled.

Table 4 shows the frequencies of hydroacoustic oscillations at initial multiplicity of 3 in three engine operating modes:  $p_2/p_1 = 220$  is the nominal mode,  $p_2/p_1 = 93.5/94$  is the case when thrust throttling leads to such an increase in the frequency of hydroacoustic oscillations that the multiplicity becomes equal to 2, and the mode  $p_2/p_1 = 51.5$ , corresponding to a decrease in the main combustion chamber's pressure by  $\sim 4.25$  times, which leads to a drop in the thrust of Raptor-2 engine by a factor of 5, and reaching the lower limit of its stable operation [23]. The discrepancy between pressure and engine thrust drops is caused by a decrease in the specific impulse of the rocket engine when it deviates from its optimal (nominal) operating mode. Estimates show [24] that the specific impulse in this extreme mode decreases by about 15 %. And hence the lower limit of the working pressure was determined.

**Table 4**

Rocket Stage Engine	$p_2/p_1$	$L_1$ (m)	$L_2$ (m)	$L_3$ (m)	$L_{eq}$ (m)	$f_n$ (Hz)	
$c = 1495$ m/s							
Starship Super Heavy Raptor-2	220	1.46	33.4 + 3.00	37.86	173	2.16	1.85/0.31
		2.93		39.33	243	1.54	
		2.01		38.41	202	1.85	1.85
	93.5	1.46		37.86	116	3.23	2.78/0.45
		2.93		39.33	160	2.33	
	94	2.01		38.41	134	2.78	2.78
	51.5	1.46		37.86	88.7	4.21	3.65/0.56
		2.93		39.33	121	3.09	
		2.01		38.41	102	3.66	3.66

To the pair of methane pipelines considered above with a length ratio of  $\sim 1:2$ , in Table 4 a technically impossible option is added everywhere when their lengths are equal. In this case, the frequency of oscillations in the circuit is the same. The most important result of comparing these two length ratios is that it practically does not affect the change in the frequency of hydroacoustic oscillations when the engines are throttled. The transition to a new multiplicity occurs, in essence, on the same modes of their operation, and this is the key issue of all further analysis.

The same can be seen in Table 5 for the case when the initial multiplicity is 4. Again in the middle group of parameters at  $p_2/p_1 = 122$ , corresponding to the output to the multiplicity of 3, the frequency change does not depend on the ratio of methane pipelines' lengths in the pair of combustion chamber and nozzle cooling circuits.

**Table 5**

Rocket Stage Engine	$p_2/p_1$	$L_1$ (m)	$L_2$ (m)	$L_3$ (m)	$L_{eq}$ (m)	$f_n$ (Hz)	
$c = 1495$ m/s							
Starship Super Heavy Raptor-2	220	2.25	33.4 + 3.00	38.65	214	1.75	1.50/0.25
		4.47		40.87	299	1.25	
		3.09		39.49	249	1.50	1.50
	122	2.25		38.65	157	2.33	2.00/0.33
		4.47		42.08	224	1.67	
		3.09		40.81	187	2.00	
	51.5	2.25		38.65	107	3.48	3.01/0.48
		4.47		40.87	148	2.53	
		3.09		40.81	124	3.01	3.01

But, apparently, the most interesting result in Table 5 is shown in the last group of data at  $p_2/p_1 = 51.5$ , that is, at the boundary of the engine operating mode. It exactly corresponds to the mode of transition to a multiplicity of 2. And this is not a mere accident. As mentioned earlier, in the hydroacoustic systems under consideration with large or very large pressure rises, with a constant geometry, their frequency is inversely proportional to the square root of the pressure rise in pump with a high degree of accuracy. Therefore, when the  $p_2/p_1$  parameter decreases by 4 – 4.25 times, which approximately corresponds to reaching the limit of Raptor-2 operating mode in terms of thrust, the carrier frequency in the hydroacoustic circuit decreases by 2 times, and the multiplicity of 4 turns into a much more

prone to excitation multiplicity 2. So such a decrease in pressure in the combustion chamber of the engine in flight, if a multiplicity of 4 is realized in its nominal operating mode, would be very dangerous for the engine due to very rapid growth of self-oscillations in this mode.

So, from analysis of the data presented in Table 4, it follows that with the initially existing in the system at nominal mode of engine operation, frequency ratio of 3 for two processes that jointly create self-oscillations of Pogo-type, the transition to the ratio of 2 occurs when the engine is throttled approximately at values  $\sim 0.4$  in thrust or at 0.425 in pressure from their nominal value. Therefore, if the rocket control system, in response to excitation and the growth of self-oscillations, begins to reduce the engines thrust, then the frequency of hydroacoustic oscillations will begin to increase, and they will move away from the multiplicity of 3. The oscillation amplitude will decrease, and the rocket acceleration will decrease. On the graph shown in Fig. 2, there will be a spike down. But at the same time, the oscillation system approaches the multiplicity 2, which is much more prone to excitation, and at some point will be able to reach it. Then the oscillation amplitudes suddenly begin to grow rapidly, and the data on the acceleration of the rocket due to renewed strong vibrations show a strong spike up on the graph. After that, a change in frequency with a further – anyway – a decrease or increase in thrust will again interrupt the development of the self-oscillation process.

With a starting multiplicity of 4, instead of one point of superspikes occurrence, there can already be two of it, and the last is located directly in the vicinity of the lower boundary of the engine operating mode, and superspikes, although of different intensity, should have been two in each excitation cycle. All this could well be seen on the acceleration graphs.

But this idealized description of the development of Pogo oscillations can be heavily adjusted due to engine characteristics. Although closed-circuit rocket engines, to which Raptor-2 belongs, "have great dynamism" [8], there is still a delay between the command to change their mode of operation and their actual entry into this mode. Therefore, it is possible to imagine such a scenario of the control system's struggle with oscillations of Pogo-type: after the development of Pogo to a certain level in the nominal mode of the engines operation, the control system begins to quickly reduce thrust, the oscillatory circuit leaves the vicinity of the first frequency multiplicity (3 or 4, depending on the length of the fuel lines), and amplitude of the oscillations decreases to the level when the control system sends a signal to return the engine operation to nominal. But due to inertia of transient processes, thrust of the engines and pressure in the fuel system continue to decrease for some time. Due to the rapid decrease in thrust and amplitude of oscillations, a downward spike occurs, but here the oscillatory circuit will be close the point of the second multiplicity (2 or 3), the excitation in which is much stronger than in the first. There is a sharp, short and powerful spike upwards, but, finally, the beginning increase in thrust brings the system to lower frequencies, where influence of this second multiplicity stops, and the system briefly reaches nominal mode of engines operation. After which the oscillatory cycle begins to slowly develop again in the vicinity of the first multiplicity point, but already, sometimes with a smaller number of operating engines due to shutdown of some of them at the moment of maximum vibrations excitation.

It seems that such a scenario most accurately describes the pattern of Starship oscillations presented in Fig. 2. With this development option, at starting multiplicity of 3 or 4, the superspike cycles differ only in degree of thrust throttling at which they are completed. Deeper throttling, corresponding to the initial multiplicity of 3, is 0.4 in terms of thrust versus  $\sim 0.5$  at initial multiplicity of 4. Due to the fact that the spikes in the acceleration drop lead to their almost zero values, it should be assumed that, most likely, a process with the transition oscillations of Pogo-type from a multiplicity of 3 to a multiplicity of 2. This is the second argument in favor of the fact that the initial multiplicity of hydroacoustic oscillations is 3.

## Conclusions

1. This study shows that during the first test flight of Starship on April 20, 2023, intense Pogo oscillations with a frequency of about 6 Hz occurred in it, activated by hydroacoustic oscillations in methane supply pipelines of engines with a frequency of 1.5 – 2 Hz and a multiplicity of 3 or 4, which, by influencing the thrust of the engines, closed a positive feedback loop with the longitudinal oscillations of the hull.
2. The control system parried these oscillations, quickly reducing engines thrust when a certain level of oscillation was reached, wherein the oscillatory circuit left Pogo excitation zone, and the control system sent a signal to return the thrust to its original level.
3. But, due to inertia of the transient processes, the thrust of the engines and the pressure in the fuel system continued to decrease for some time, a downward spike appeared on the acceleration diagram, and the oscillatory circuit fell into the multiplicity zone, respectively, 2 or 3.

4. In this case, there was a sharp increase in the amplitude of the oscillations, and the second element of the superspike appeared on the acceleration diagram – an upward spike.
5. After that, the thrust of the engines finally began to grow, and due to exit of frequencies from the second excitation zone, Pogo-type oscillations died out.
6. The system reached the nominal mode of engines operation, after which the oscillatory cycle began to slowly develop again in the vicinity of the first multiplicity point, but sometimes with fewer working engines.
7. Thus, there was a cycle of at least 10 fragments with superspikes, duration of each fragment was about 12 seconds, and during each fragment there were ~ 70 Pogo oscillations, until control over Starship was finally lost due to very strong oscillations of its structure and accompanying phenomena, and it was destroyed.
8. A higher probability of self-oscillations at a lower multiplicity, as well as a greater depth of acceleration drop on the first spike, testifies in favor of the fact that the initial multiplicity of hydroacoustic oscillations was 3, and length of methane pipeline high-pressure sections in Raptor-2 engine corresponds to the so-called "short" version.
9. Until the problem described in this work will be eliminated, it is impossible to talk not only about a manned flight to Mars, but also about more or less regular exits to near-Earth orbit.

### Literature

1. K. Chang – SpaceX Rocket Struggled to Self-Destruct as It Spun Out of Control. *The New York Times*, 29 April 2023 // <https://www.nytimes.com/2023/04/29/science/elon-musk-spacex-starship.html>
2. FAILURE: SpaceX Starship 1st Flight. *NASASPACEFLIGHT*, Reply #263, 30 April 2023 // <https://forum.nasaspaceflight.com/index.php?topic=58669.msg2483001#msg2483001>
3. Topic: SpaceX Raptor engine. *NASASPACEFLIGHT*, Reply #2109, 23 April 2023 // <https://forum.nasaspaceflight.com/index.php?topic=53555.2100>
4. Starship Flight Test. *SpaceX*, 20 April 2023 // <https://www.youtube.com/watch?v=-1wciIQ58hI>
5. FAILURE: SpaceX Starship 1st Flight. *NASASPACEFLIGHT*, Reply #186, 21 April 2023 // <https://forum.nasaspaceflight.com/index.php?topic=58669.180>
6. FAILURE: SpaceX Starship 1st Flight. *NASASPACEFLIGHT*, Reply #161, 20 April 2023 // <https://forum.nasaspaceflight.com/index.php?topic=58669.msg2477879#msg2477879>
7. SpaceX Starship sequence of events // <https://www.funkystuff.org/spacex-starship-sequence-of-events/>
8. B. I. Rabinovich – Instability of liquid-propellant rockets and space vehicles and some fragments of the history of combating it. *Preprint IKI RAS*, 2006, 40 p. // <http://www.iki.rssi.ru/books/2006rabinovich.pdf> (in Russian)
9. Apollo 13. Day 1, part 1: Launch and Reaching Earth Orbit. *Apollo Flight Journal*. National Aeronautics and Space Administration, NASA History Division, 6 April 2020 // [https://history.nasa.gov/afj/ap13fj/01launch\\_ascent.html](https://history.nasa.gov/afj/ap13fj/01launch_ascent.html)
10. V. Kh. Arm, V. L. Okulov, and I. M. Pylev – Instability of penstocks. *Reports of the Academy of Sciences, Energy*, 1995, **341**, no 4 (in Russian)
11. Yu. I. Lobanovsky – Excitation criterion of hydroacoustic self-oscillations in hydro stations penstocks. *Synerjetics Group*, 10.01 – 10.02.2010, 41 p. // <http://synerjetics.ru/article/excitation.htm> (in Russian)
12. Yu. I. Lobanovsky – Self-oscillations in penstocks of hydroelectric power stations and Sayan catastrophe. "Hydropower of Ukraine", N 3 – 4, 2013, 11 p. // <http://www.synerjetics.ru/article/autooscillations.htm> (in Russian)
13. Rocketdyne F-1. *Wikipedia* // [https://en.wikipedia.org/wiki/Rocketdyne\\_F-1](https://en.wikipedia.org/wiki/Rocketdyne_F-1)
14. Rocketdyne J-2. *Wikipedia* // [https://en.wikipedia.org/wiki/Rocketdyne\\_J-2](https://en.wikipedia.org/wiki/Rocketdyne_J-2)
15. K. D. McCutcheon – U.S. Manned Rocket Propulsion Evolution. Part 8.10: The Saturn V S-IC Stage. 3 August 2022 // <https://www.enginehistory.org/Rockets/RPE08.10/RPE08.10.shtml>
16. K. D. McCutcheon – U.S. Manned Rocket Propulsion Evolution. Part 8.20: The Saturn V S-II Stage. 3 August 2022 // <https://www.enginehistory.org/Rockets/RPE08.20/RPE08.20.shtml>
17. Anon. – Turbopump Systems for Liquid Rocket Engines. *NASA SP-8107*, 1 August 1974 // <https://ntrs.nasa.gov/citations/19750012398>
18. V. V. Sychev, A. A. Vasserman, A. D. Kozlov, et al. – Thermodynamic properties of oxygen. Moscow, Standards Publishing House, 1981, 304 p. // <https://nauca.ru/ref/Термодинамические-свойства-кислорода-ГСССД.1.pdf> (in Russian)
19. N. E. Zhukovsky – On hydraulic shock in water pipes. M - L, Gostekhizdat, 1949 (in Russian)
20. B. I. Klyachin – Low-frequency noise field of Lake Baikal. *Ocean researches*, **46**, no 2, 2018, p. 28 – 36 // <https://jor.ocean.ru/index.php/jor/article/view/147/60> (in Russian)
21. Methane liquid and gaseous. GOST R 8.1020-2023. Introduction date 12.01.2023 // <https://gostassistant.ru/doc/60d40a0b-6c4c-4939-acb8-70c4b682839a> (in Russian)



22. SpaceX Starship. *Wikipedia* // [https://en.wikipedia.org/wiki/SpaceX\\_Starship](https://en.wikipedia.org/wiki/SpaceX_Starship)
23. SpaceX Raptor. *Wikipedia* // [https://en.wikipedia.org/wiki/SpaceX\\_Raptor](https://en.wikipedia.org/wiki/SpaceX_Raptor)
24. Yu. I. Lobanovsky – Conservation laws and phenomenology of rocket engines. *Synerjetics Group*, 30.06.2008, 21 p. // [http://www.synerjetics.ru/article/rocket\\_engines.pdf](http://www.synerjetics.ru/article/rocket_engines.pdf) (in Russian)
25. N. S. Anofrikova – Vibrations of elastic rods. Part I. Saratov State University, Textbook, 2014, 45 p. // [http://elibrary.sgu.ru/uch\\_lit/1111.pdf](http://elibrary.sgu.ru/uch_lit/1111.pdf) (in Russian)
26. K. D. McCutcheon – U.S. Manned Rocket Propulsion Evolution. Part 9.10: The Apollo Launch Escape System. 4 August 2022 // <https://www.enginehistory.org/Rockets/RPE09.10/RPE09.10.shtml>
27. 7075 aluminium alloy. *Wikipedia* // [https://en.wikipedia.org/wiki/7075\\_aluminium\\_alloy](https://en.wikipedia.org/wiki/7075_aluminium_alloy)
28. AISI Type 304L Stainless Steel. *ASM Specification Metals Inc.* // <https://asm.matweb.com/search/SpecificMaterial.asp?bassnum=MQ304L>
29. I. Afanasiev – N-1: Top secret. *Wings of Motherland*, no 9 – 11, 1993 // <https://epizodyspace.ru/bibl/k-r/1993/9-n-1.html> (in Russian)
30. Yu. I. Lobanovsky – Summary data on detected hydroacoustic incidents. *Synerjetics Group*, 05.01.2015, 4 p. // [http://www.synerjetics.ru/article/aggregated\\_data.pdf](http://www.synerjetics.ru/article/aggregated_data.pdf) (in Russian)

Moscow,  
05.10.2023

Yu. I. Lobanovsky